Imperial College London

Imperial College London
Department of Mathematics

Second year project **Group 19**

Gangs and Graffiti: A Statistical Mechanical Approach

Authors:
Sanjiv Dutt
Bhagyata Kinger
Alina Leidinger
Lana Mineh

Supervisor:
Dr. Yanghong Huang

June 2015

Abstract

Gangs. Graffiti. The Ising Model. How are they related? We demonstrate how the Ising Model, renowned for its use in Statistical Mechanics, is implemented to investigate the interaction between gangs and graffiti. We apply a variety of mathematical techniques and approaches including Markov Chains, Monte Carlo Methods and Mean Field Theory. Furthermore, adapting the model to include factors such as socioeconomic stability and social influence could prove to be useful in understanding, monitoring and controlling of gang activity.

Contents

1 Introduction **1**

2 The Ising Model **3**
2.1 Background . . . 3
2.2 2-Dimensional Ising Model . . . 3
2.3 Application to Gangs and Graffiti . . . 4
2.4 Adaptation of Classical Ising Model . . . 5
2.5 Reduced Model . . . 6

3 The Metropolis Algorithm **7**
3.1 Metropolis Algorithm in a General Setting . . . 7
3.2 Metropolis Algorithm for the Ising Model . . . 8
3.3 Metropolis Algorithm for Gangs and Graffiti . . . 8

4 Mean Field Theory **16**
4.1 The Standard Approach . . . 16
4.1.1 Mean Field Theory in the Ising Model . . . 16
4.1.2 Application to Gangs and Graffiti . . . 17
4.2 An Alternative Approach . . . 20
4.2.1 Background . . . 20
4.2.2 Application to the Reduced Model . . . 20

5 Simulations **24**
5.1 Phase Transition . . . 24
5.2 Gang Fraction . . . 27
5.3 Energy of the System . . . 28

6 Conclusion **29**

Bibliography **30**

A Code **31**
A.1 Main Function to Calculate Gang Fractions . . . 31
A.2 C Code to run the Metropolis Algorithm . . . 32
A.3 Part of the Code for the Initial Configuration of the Grid . . . 34

Chapter 1

Introduction

"Go down deep enough into anything and you will find mathematics."

– Dean Schlicter

There remain areas where there is lack of mathematical research. The study of the mathematics of gangs is one such area of life that remained untouched by the academia in Mathematics until recently. It was not until 2012 that the study "Territorial Developments Based on Graffiti: A Statistical Mechanics Approach" was conducted in California [1].

When Ising was working on his PhD thesis in 1924 and solved the one dimensional model, it is likely he did not forsee the applications of his model outside ferromagnetism. The two dimensional Ising Model has been applied to many different fields of research. The lattice structure has been applied to areas in physical chemistry such as crystallography, in biology for modelling DNA and recently to model the interaction between gangs and graffiti.

It seems natural that this application of the Ising Model to gangs and graffiti was developed in California, where gang culture is more prevalent than in the United Kingdom. Last year, in the project "Ising Model for Gangs and Graffiti", an initial analysis was performed into this culture in the UK [2]. We aim to take their research further in this report.

Figure 1.1: Graffiti [3]

While gang activity in the UK is considered to be lower than in the USA, there is no doubt that there is a gang presence in the UK where guns are replaced by knives. Police have identified 170 gangs that operate in London [4], with many more around the country. In the UK, youth involvement in gangs remains a high concern with children as young as 10 being parts of gangs. The UK riots in August 2011 are an example of the power that gangs have in turning a peaceful protest to a violent riot (pictured below).

Figure 1.2: UK Riots 2012 [5]

In this report, we will first study the background of the Ising Model and then discuss its application to the relationship between gangs and graffiti in Chapter 2. Then in Chapter 3 we apply the Metropolis algorithm, a prominent algorithm in Markov Chain Monte Carlo Methods, to the Ising model. We then apply this theory to find Markov Chain transition matrices and then evaluate the efficiency of each of these matrices. Moving forward in Chapter 4, we will discuss how Mean Field Theory can be applied to our adaptation of the Ising model. Finally, in Chapter 5, we will look at simulations and make deductions about the ways in which to minimise gang activity.

Chapter 2

The Ising Model

2.1 Background

The Ising Model was first proposed by Wilhelm Lenz in 1920 in his research into ferromagnetism. Lenz subsequently suggested the model to his then student Ernst Ising as a potential area for further investigation in his doctoral thesis, which was published in 1924. Originally Ising used the model to replicate the behaviour of a linear chain (1-dimensional) of magnetic moments which can have two configurations – either up or down – and are influenced by interactions between their adjacent particles. This research was then extended to explore the area of "spontaneous magnetization" which was the core investigation of Ising's thesis [6].

The Ising model is particularly impressive due to its simplicity and ability to give firm and quantitative indications. It studies microscopic short range interactions between neighbouring particles that can produce phase transitions [7]. However this was not always the case. Originally Ising determined in his thesis that in the 1-dimensional case no phase transition occurs, and consequently concluded that this held for higher dimensions. Fortunately this error was rectified by L. Onsager in 1944 who proved phase transition is exhibited in a 2-dimensional model [8].

Indeed the model has now been extended to higher dimensions with the aid of many other techniques, including mean field theories, transfer matrices, series expansions, Monte Carlo simulations and renormalization groups [9]. Further research into this field has yielded much success in the study of critical phenomena. It has also aided in many interesting developments in the theory of Markov Chains, information theory and random walks [7]. It is sensible to adapt our model to investigate the patterns and tendencies of gang activity and the associated graffiti, which will be introduced and studied further on in the report.

2.2 2-Dimensional Ising Model

Consider a two dimensional system on a finite square lattice $\Lambda \subset \mathbb{Z}^2$. The spin at each site $i \in \Lambda$ is denoted by σ_i and can take one of the two configurations $\{+1, -1\}$ and conforms to an external magnetic field, h_i. This is equivalent to our red upward pointing arrow and

blue downward pointing arrow in Figure 2.1. In our model we work under the assumption that only short-range interactions and any influences from the external field contribute to the energy level of the system, again this can be seen by the faded out arrows in Figure 2.1. From this we can form the Hamiltonian, $\mathcal{H}$ of the system, which dictates the dynamics of the overall energy of the system [6].

$$-\mathcal{H}(\sigma) = \sum_{\langle i,j \rangle} J_{ij}\sigma_i\sigma_j + K\sum_i h_i\sigma_i. \tag{2.1}$$

Here, the first sum is over the four nearest neighbours of a site in the lattice, denoted $\sum_{\langle i,j \rangle}$, and the second sum is over all lattice sites. $\sigma = (\sigma_i)_{i\in\Lambda}$ is the spin configuration of a particular lattice site whilst the parameters J_{ij} and K correspond to the interaction between two adjacent sites, i and j and the magnetic moment of the system respectively [10].

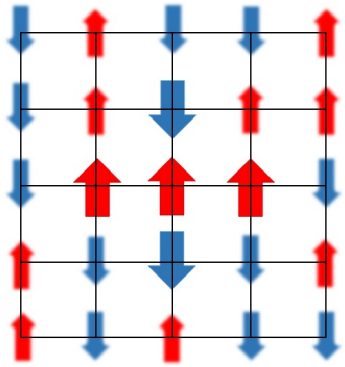

Figure 2.1: A 2D square-lattice Ising model

Note:

$$J_{ij} = \begin{cases} J, & \text{if } i,j \text{ are nearest neighbours} \\ 0, & \text{otherwise.} \end{cases} \quad [11]$$

For a ferromagnet, J is positive and a large proportion of nearest neighbour pairs tend to have parallel alignment ($\sigma_i = \sigma_j$). This leads to the ferromagnet having a lower energy level than a non-magnetised system. Likewise, if Kh is positive this leads to the alignment of magnetic moments parallel to the external magnetic field and consequently a low energy level [2, 6].

This is consistent with the idea that a high energy level implies that there exist a lot of fluctuations in the overall system. Sites are switching between states rapidly and there is an instability in the system. However, at a lower energy level the Hamiltonian is more negative, and the overall system is tending towards a steady state.

2.3 Application to Gangs and Graffiti

Our project aims to present a model that describes the distribution and impact of two rival gangs, hereafter referred to as the red and blue gang, in a community. Both of these gangs

manage their own organisation and are influenced by external factors, such as socioeconomic stability, education and social influence.

In particular, we refer to members of each gang as agents. We deliberately avoid including direct interactions between agents, however the rivalry between gangs to mark territories with graffiti as a sign of dominance is taken into account. Agents are then attracted to sites with graffiti of their same color, and abstain from entering locations marked by their opponents. Additionally, this graffiti tagging creates a sphere of influence to join or leave these gangs. Considering all these elements provides a platform to investigate the role of graffiti and the influence it has on a community [1].

It is natural to associate the agent spin σ_i to the gang affiliation of a specific agent. However this fails to acknowledge the potential for certain sites to be gang neutral. Hence, we adapt our model to consider such a situation whereby gangs are in competition to claim such sites.

2.4 Adaptation of Classical Ising Model

Note: The report by A. Barbaro [1], is used widely in the next few sections as a basis of derivation and explanation of our model.

Thus we adapt the Classical Ising Model to fit with our newly included parameters. Define a spin system on a finite lattice $\Lambda \subset \mathbb{Z}^2$. Here, the spin at each site $i \in \Lambda$ is denoted by $s_i = (\eta_i, g_i)$, where η_i corresponds to the agent spin and g_i represents the graffiti field. We allow the agent spin to take one of the following values: $\{0, \pm 1\}$; $\eta_i = 1$ if the agent at site i belongs to the blue gang, $\eta_i = +1$ if the agent is a red gang member and $\eta_i = 0$ if there is no agent. The graffiti field, g_i takes all values in $\mathbb{R}$, where $g_i > 0$ indicates an excess of red graffiti, equivalently $g_i < 0$ corresponds to an excess of blue graffiti.

Now we introduce the Graffiti-Interaction GI-Hamiltonian,

$$-\mathcal{H}(\underline{s}) = J \sum_{\langle i,j \rangle} \eta_i g_j + K \sum_i \eta_i g_i + \alpha \sum_i \eta_i^2 - \lambda \sum_i g_i^2. \tag{2.2}$$

The interpretation of the parameters is as follows:

1. $\underline{s}$ is a given configuration on the lattice Λ, i and j indicate sites on the lattice and as before $\sum_{\langle i,j \rangle}$ denotes sum over nearest four neighbours of a particular site.
2. J denotes the likelihood of a neighbouring agent to align its spin with the spin of the agent at site i. To ensure consistency we require $J > 0$ to fit with our model.
3. K corresponds to the external magnetic field. The larger the magnitude, the higher the probability of the spins aligning. In the context of our model, this indicates the likelihood of a certain gang member to be in close range to another agent of the same gang. Again tacitly K is required to be > 0
4. $\alpha \in \mathbb{R}$ represents the inclination for an agent to occupy territories regardless of colour. If $\alpha >> 1$ there is a strong tendency for an agent to claim the turf, whereas if $\alpha << 1$ there is a natural sparsity of gangs in particular areas.

5. λ constitutes the social influence, whether it be socioeconomic stability, law enforcement presence or the literacy rate. We require $\lambda > 0$, and as the value of λ increases the concentration of graffity decreases [1, 2].

Note: illustrations of the consequences of inconsistency in our model, for example, taking parameters J, K to be < 0 can be found in last years report [2]. Contextually $J < 0$ is unrealistic as it implies that neighbouring territories have a higher likelihood to be occupied by rival gangs. Furthermore, $K < 0$ is counter intuitive as it indicates that rival gangs are more likely to inhabit turf that has been marked by opposing gang members.

2.5 Reduced Model

Ideally we would like to reduce and simplify the model to resemble the Classical Ising model. This involves optimising the model we have in (2.2) according to certain constraints. These calculations and amendments were performed in last year's report [2]. Thus, in the remainder of this report we assume the results established in last year's report.

Our reduced Hamiltonian $\mathcal{H}_r$ is as follows:

$$-\mathcal{H}_r(\underline{s}) = J_1 \sum_i \eta_i^2 + J_2 \sum_{\langle i,j \rangle} \eta_i \eta_j + J_3 \sum_{\langle\langle i,j \rangle\rangle_1} \eta_i \eta_j + J_4 \sum_{\langle\langle i,j \rangle\rangle_2} \eta_i \eta_j, \tag{2.3}$$

where

$$J_1 = \alpha + \frac{4J^2 + K^2}{4\lambda}, \quad J_2 = \frac{JK}{\lambda}, \quad J_3 = \frac{J^2}{2\lambda}, \quad J_4 = \frac{J^2}{\lambda}.$$

Notice that for each site i we now consider 12 of its nearest neighbours. The four blue neighbours are the same as those considered previously. However, now we also include the influences from the diagonal neighbours (green) and that of the neighbours two sites away (red) represented in Figure 2.2. These are reflected by the summations in the revised Hamiltonian.

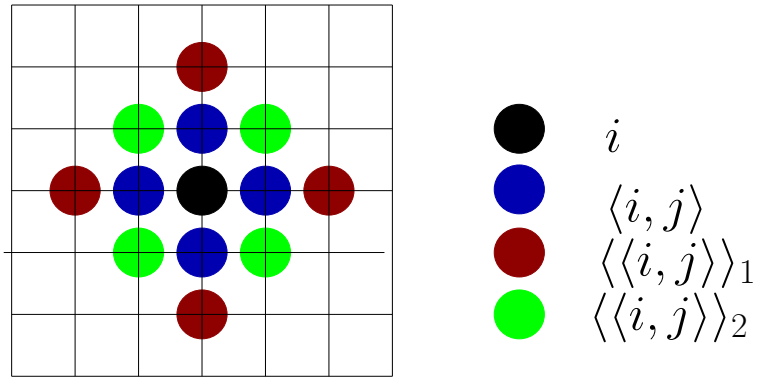

Figure 2.2: Different types of nearest-neighbours [2]

Additionally, the reduced model does not take into account the graffiti field g_i. This enables the study of purely gang-gang interaction η, without the effects of graffiti tagging in specific neighbourhoods.

In the following chapters, simulations and analysis are based solely on the reduced model.

Chapter 3

The Metropolis Algorithm

3.1 Metropolis Algorithm in a General Setting

The Metropolis Algorithm tackles the problem of sampling from a given probability density p_x that might be very difficult to sample from directly. It constructs a Markov Chain that leads to an equilibrium distribution π s.t. $\pi(\mathrm{x}) = p_x$ [12]. One way of realising this is for probabilities to fulfill the condition of detailed balance.

$$\pi(\theta)p(\theta,\phi) = \pi(\phi)p(\phi,\theta). \tag{3.1}$$

Here, θ, ϕ are two configurations of the system, $p(\theta,\phi)$ and $p(\phi,\theta)$ are transition kernels representing the probabilities of moving from θ to ϕ and ϕ to θ, respectively.
Formally, the transistion kernel $p(x,A)$ for $x \in S$ (sample space), $A \subset S$, is defined to have the following properties:

- $\forall x \in S, p(x,\cdot)$ is a probability distribution on S.
- $\forall A \subset S$, we can evaluate $x \mapsto p(x,A)$.

In the discrete case, $p(x,\{y\}) = p(x,y)$ and we have a probability that satisfies all the usual axioms [12]. In the continuous case, this does not hold as $p(x,\{y\}) = 0$. This is why we cannot obtain a transistion matrix, unlike in the discrete case, so we consider transition kernels [12].
In the case of the Metropolis algorithm,

$$p(\theta,\phi) = q(\theta,\phi)\alpha(\theta,\phi),$$

where q is any transition kernel and α is a so called acceptance probability [12].
A prevalent expression for α is

$$\alpha(\theta,\phi) = min\left\{1, \frac{\pi(\phi)q(\phi,\theta)}{\pi(\theta)q(\theta,\phi)}\right\},$$

which makes it the Metropolis Algorithm.

3.2 Metropolis Algorithm for the Ising Model

If we apply the Metropolis Algorithm to the Ising Model, we are considering an $n \times n$ lattice consisting of spins that can be in one of two possible states. Starting with an initial configuration, we pick one spin at a time deciding whether to flip it or not. The algorithm is designed in such a way that we reach an equilibrium and that the vector of probabilities associated with the equilibrium is distributed according to the Boltzmann distribution [13].

1. Assume an initial configuration of our $n \times n$ lattice, θ (more on the different possibilities below).
2. Randomly select one out of the n^2 spins, spin k, say. The probabilities of selecting one particular spin are all equal i.e. equal to $\frac{1}{n^2}$.
3. We try to decide whether to flip spin k. Let the current configuration of the lattice be θ and the configuration with k flipped be ϕ. Let the total energy of the system at θ and ϕ be E_θ, E_ϕ respectively. As our probabilities should be Boltzmann distributed at equilibrium and because selection probabilities are all equal (see 2.), rearranging equation (3.1):

$$\frac{p(\theta,\phi)}{p(\phi,\theta)} = \frac{q(\theta,\phi)\alpha(\theta,\phi)}{q(\phi,\theta)\alpha(\phi,\theta)} = \frac{\alpha(\theta,\phi)}{\alpha(\phi,\theta)} = e^{-\beta(E_\phi - E_\theta)}.$$

   Here $\beta^{-1} = \kappa T$, the thermal energy of the system where T is temperature and κ is the Boltzmann Constant [13]. The condition still leaves us some scope in deciding what the acceptance probablities should be. In order to increase computational speed [13], we take

$$p(\theta,\phi) = \begin{cases} e^{-\beta(E_\phi - E_\theta)} & \text{if } E_\theta < E_\phi \\ 1 & \text{otherwise.} \end{cases}$$

   This means that we always accept a move if it decreases the energy of the system, because we need to reach a steady state. If a move increases the energy of our system, we generate a uniform random number r between 0 and 1 and accept the move if r $< e^{-\beta((E_\phi - E_\theta)}$ and reject it otherwise.

We repeat 2 and 3 for a number of iterations.
Two different popular possibilities for initial configurations are either choosing states of the spins at random, which corresponds to $T = +\infty$, or having all spins in the same state, which corresponds to $T = 0$ [13].

3.3 Metropolis Algorithm for Gangs and Graffiti

We apply the Ising Model to gangs and graffiti by considering our n x n lattice as an area in which we want to investigate gang dominance. Every spin in the lattice can be in one of three states -1, 0, 1 representing that area either being claimed through graffiti by the blue gang, neutral or claimed by the red gang. Let the energy states associated with the three states be E_1, E_2, E_3. Without loss of generality assume $E_1 \leq E_2 \leq E_3$.
We try to find a **transition matrix** that represents our Markov Chain. Conditions on the

transition matrix are that the columns add to one, the entries are non-negative i.e. represent probabilities and thirdly that we have

$$v_1 = \begin{pmatrix} e^{-E_1} \\ e^{-E_2} \\ e^{-E_3} \end{pmatrix},$$

our only eigenvector with eigenvalue 1. This implies that v_1 represents our probability distribution at equilibrium which is the Boltzmann distribution and that this is the only local equilibrium so that we don't get stuck in a different equilibrium when doing our simulation.

In the classical Ising model we only have two states $E_1 \leq E_2$ and in this case the most basic transition matrix would be the following:

$$\begin{pmatrix} 1 - e^{-(E_2 - E_1)} & 1 \\ e^{-(E_2 - E_1)} & 0 \end{pmatrix}.$$

We now try to extend this to three states.

1. Inspired by the 2×2 matrix we let

$$Q = \begin{pmatrix} \star & \star & 1 \\ \star & \star & 0 \\ \star & \star & 0 \end{pmatrix},$$

so we always accept a move from the highest to the lowest energy level. Now we fill in the blanks. We try to have as many zeros and ones as possible, because this makes computation easier.

Is it possible to have two zeros in the second column?

(a) Let

$$Q = \begin{pmatrix} q_{11} & 1 & 1 \\ q_{21} & 0 & 0 \\ q_{31} & 0 & 0 \end{pmatrix},$$

our condition on the eigenvector gives

$$q_{12} = e^{E_1 - E_2}, \ q_{13} = e^{E_1 - E_3}$$

and because columns add to one:

$$q_{11} = 1 - e^{E_1 - E_2} - e^{E_1 - E_3}$$

. However, this could be negative if $E_1 \leq E_2 \leq E_3$ are all close to zero, so we can rule this case out.

(b) Let

$$Q = \begin{pmatrix} q_{11} & 0 & 1 \\ q_{21} & 1 & 0 \\ q_{31} & 0 & 0 \end{pmatrix}.$$

We apply the conditions and obtain

$$q_{11} = 1 - e^{E_1 - E_3}, \quad q_{12} = 0, \quad q_{13} = e^{E_1 - E_3}$$

. However, in this case we can check that

$$\begin{pmatrix} e^{-E_1} \\ 0 \\ e^{-E_3} \end{pmatrix}, \quad \begin{pmatrix} 0 \\ e^{-E_2} \\ 0 \end{pmatrix}$$

are both eigenvectors with eigenvalue 1, meaning that we can end up in the wrong equilibrium when doing our simulations which is undesirable.

(c) Let

$$Q = \begin{pmatrix} q_{11} & 0 & 1 \\ q_{21} & 0 & 0 \\ q_{31} & 1 & 0 \end{pmatrix},$$

Then the last equation for our eigenvector is

$$q_{31}\, e^{-E_1} + e^{-E_2} = e^{-E_3},$$

which means that $q_{31} \leq 0$

Therefore we cannot have two zeros on the second column. Let's try one zero on the second column.

(d) Let

$$Q = \begin{pmatrix} 1-a-b & 0 & 1 \\ a & 1-c & 0 \\ b & c & 0 \end{pmatrix},$$

so that $a + b \leq 1, \quad 0 < c < 1$
Can we get a zero in the first column?
The second and the third equation for the eigenvector give

$$a = c\, e^{E_1 - E_2}, \quad b = e^{-E_3} - ce^{-E_2}.$$

The first equation is linearly dependent. $a + b = 1$ is not possible, as this implies $e^{-E_1} = e^{-E_3}$, so $q_{11} \neq 0$.
As $0 < a = c\, e^{E_1 - E_2} < 1$, to get a zero in the first column we need to set $b = 0$.
Hence one possible transition matrix is

$$Q = \begin{pmatrix} 1 - e^{E_1 - E_3} & 0 & 1 \\ e^{E_1 - E_3} & 1 - e^{E_2 - E_3} & 0 \\ 0 & e^{E_2 - E_3} & 0 \end{pmatrix}. \tag{3.2}$$

(e) Let

$$Q = \begin{pmatrix} 1-a-b & 1-c & 1 \\ a & 0 & 0 \\ b & c & 0 \end{pmatrix}.$$

The second equation for our eigenvector implies $a = e^{E_1 - E_2}$. If $q_{11} = 0$ our first matrix equation becomes

$$(1-c)e^{-E_2} + e^{-E_3} = e^{-E_1}.$$

This could give a negative value for c if E_2, E_3 are much bigger than E_1, so we rule this case out.
However, $b = 0$ is possible. Hence,

$$Q = \begin{pmatrix} 1-e^{E_1-E_2} & 1-e^{E_2-E_3} & 1 \\ e^{E_1-E_2} & 0 & 0 \\ 0 & e^{E_2-E_3} & 0 \end{pmatrix}. \tag{3.3}$$

(f) Let

$$Q = \begin{pmatrix} 1-a-b & c & 1 \\ a & 1-c & 0 \\ b & 0 & 0 \end{pmatrix}.$$

The third equation implies $b = e^{E_1 - E_3}$.
If $a = 0$, then $c = 0$. This would give us two zeros on the second columns which we ruled out earlier.
If $1 - a - b = 0$, then $a = 1 - b = 1 - e^{E_1 - E_3}$.
Then the first eigenvector equation becomes

$$c\, e^{-E_2} + e^{-E_3} = e^{-E_1}.$$

This gives $c > 1$ if E_1 is much smaller than E_2, E_3. So having $q_{32} = 0$ is impossible [14].

We have found two transition matrices so far. Now we consider changing the third column.

2. Let

$$Q = \begin{pmatrix} \star & \star & 0 \\ \star & \star & 1 \\ \star & \star & 0 \end{pmatrix}.$$

Is it possible to have two zeros in the second column?

(a) Let

$$Q = \begin{pmatrix} 1-a-b & 1 & 0 \\ a & 0 & 1 \\ b & 0 & 0 \end{pmatrix}.$$

The equations for our eigenvector give $a = e^{E_1}(e^{-E_2} - e^{-E_3})$, which is bigger than one for E_1, E_2, E_3 very small and close together.

(b) Let

$$Q = \begin{pmatrix} 1-a-b & 0 & 0 \\ a & 1 & 1 \\ b & 0 & 0 \end{pmatrix}.$$

Then the second equation for our eigenvector gives

$$ae^{-E_1} + e^{-E_2} + e^{-E_3} = e^{-E_2} \quad \Longrightarrow \; a < 0,$$

which is impossible.

(c) Let

$$Q = \begin{pmatrix} 1-a-b & 0 & 0 \\ a & 0 & 1 \\ b & 1 & 0 \end{pmatrix}.$$

Then the last equation for the eigenvector gives

$$1 - a - b = 1 \quad \Longrightarrow \; a = b = 0$$

because $a \geq 0$, $b \geq 0$. This only fulfills the second and third equation for $E_2 = E_3$, so we can rule this case out as well.

Hence having two zeros in the second column is impossible.
Let's assume we have one zero in the second column.

(d) Let

$$Q = \begin{pmatrix} 1-a-b & 0 & 0 \\ a & 1-c & 1 \\ b & c & 0 \end{pmatrix}.$$

However, in this case we can check that

$$\begin{pmatrix} e^{-E_1} \\ 0 \\ 0 \end{pmatrix}, \quad \begin{pmatrix} 0 \\ e^{-E_2} \\ e^{-E_3} \end{pmatrix}.$$

are linearly independent eigenvectors with eigenvalue 1.

(e) Let

$$Q = \begin{pmatrix} 1-a-b & 1-c & 0 \\ a & 0 & 1 \\ b & c & 0 \end{pmatrix}.$$

The equations for our eigenvector give $a = e^{E_1}(e^{-E_2} - e^{-E_3})$, which is bigger than one for E_1, E_2, E_3 very small and close together.

(f) Let

$$Q = \begin{pmatrix} 1-a-b & c & 0 \\ a & 1-c & 1 \\ b & 0 & 0 \end{pmatrix}.$$

The third equation for our eigenvector gives $b = e^{E_1 - E_3}$. The first and the second equation are dependent, so we can choose $a = 0$. Applying the equation we obtain

$$Q = \begin{pmatrix} 1-e^{E_1-E_3} & e^{E_2-E_3} & 0 \\ 0 & 1-e^{E_2-E_3} & 1 \\ e^{E_1-E_3} & 0 & 0 \end{pmatrix}. \tag{3.4}$$

We now consider the final case; changing the third column to $\underline{e}_3$.

3. Let

$$Q = \begin{pmatrix} \star & \star & 0 \\ \star & \star & 0 \\ \star & \star & 1 \end{pmatrix}.$$

Is it possible to have two zeros in the second column?

(a) Let

$$Q = \begin{pmatrix} 1-a-b & 1 & 0 \\ a & 0 & 0 \\ b & 0 & 1 \end{pmatrix}.$$

The equations for our steady state eigenvector gives $b = 0$ and $a = e^{E_1 - E_2}$. However, in this case we can check that

$$\begin{pmatrix} 0 \\ 0 \\ e^{-E_3} \end{pmatrix}, \quad \begin{pmatrix} e^{-E_1} \\ e^{-E_2} \\ 0 \end{pmatrix}$$

are linearly independent eigenvectors with eigenvalue 1.

(b) Let

$$Q = \begin{pmatrix} 1-a-b & 0 & 0 \\ a & 1 & 0 \\ b & 0 & 1 \end{pmatrix}.$$

In this case our equations for the equilibrium eigenvector give $a = b = 0$, so we obtain the identity. However, in this trivial case, no spins on our lattice are ever spun, so we can ignore this case.

(c) Let

$$Q = \begin{pmatrix} 1-a-b & 0 & 0 \\ a & 0 & 0 \\ b & 1 & 1 \end{pmatrix}.$$

The first eigenvector equation gives us $1-a-b=1 \implies a=b=0$, as $a \geq 0$, $b \geq 0$. The second one gives us $a = e^{E_1 - E_2}$ which is a contradiction.

Can we have one zero in the second column?

(d) Let

$$Q = \begin{pmatrix} 1-a-b & 0 & 0 \\ a & 1-c & 0 \\ b & c & 1 \end{pmatrix}.$$

The first equation for our eigenvector implies $a = b = 0$ and then the third equation implies $c = 0$, so we get the identity matrix again.

(e) Let

$$Q = \begin{pmatrix} 1-a-b & 1-c & 0 \\ a & 0 & 0 \\ b & c & 1 \end{pmatrix}.$$

The third equation of our eigenvector gives

$$be^{-E_1} + ce^{-E_2} + e^{-E_3} = e^{-E_3}$$

This implies that $b = c = 0$, so we have two zeros on the second column again which we ruled out earlier.

(f) Let

$$Q = \begin{pmatrix} 1-a-b & c & 0 \\ a & 1-c & 0 \\ b & 0 & 1 \end{pmatrix}.$$

The last eigenvector equation gives $b = 0$. The first two equations are dependent and give $a = c\, e^{-E_2+E_1}$. However, for arbitrary a, c $(0 < c < 1)$, we can find two linearly independent eigenvectors with eigenvalue 1. For example for $c = \frac{1}{2}$, these might be

$$\begin{pmatrix} 0 \\ 0 \\ e^{-E_3} \end{pmatrix}, \quad \begin{pmatrix} e^{-E_1} \\ e^{-E_2} \\ 0 \end{pmatrix}.$$

Hence, we cannot find a "simple" transition matrix with the third column being

$$\begin{pmatrix} 1 \\ 0 \\ 0 \end{pmatrix}.$$

Hence, we have found three simple transition matrices in total: (3.2), (3.3), (3.4).
We now look at the remaining eigenvalues for the three matrices to show that their absolute values are less than 1. For (3.2) and (3.4), these are actually identical.
The characteristic polynomial is:

$$p(\lambda) = (\lambda - 1)(\lambda^2 + (e^{E_2 - E_3} + e^{E_1 - E_3} - 1)\lambda + e^{E_1 + E_2 - 2E_3}) = (\lambda - 1)q(\lambda).$$

The two roots of q are

$$\lambda_\pm = \frac{1}{2}\Big(- e^{E_1-E_3} - e^{E_2-E_3} + 1 \\ \pm \sqrt{e^{2E_2-2E_3} - 2e^{E_1+E_2-2E_3} + e^{2E_1-2E_3} - 2e^{E_2-E_3} - 2e^{E_1-E_3} + 1}\Big).$$

If both roots are complex then

$$| \lambda_+ |^2 = | \lambda_- |^2 = \lambda_+\lambda_- = e^{E_1+E_2-2E_3},$$

which is less than 1.
If both eigenvalues are real,

$$\lambda_+ + \lambda_- = 1 - e^{E_2-E_3} - e^{E_1-E_3},$$

which is contained in $(-1, 1)$.
Also note that $q(1) > 0$, $q(-1) > 0$. Hence $\lambda_\pm$ must be in $(-1, 1)$.

For (3.3), the characteristic polynomial is:

$$p(\mu) = (\mu - 1)(\mu^2 + e^{E_1-E_2}\mu + e^{E_1-E_3}) = (\mu - 1)q(\mu).$$

The roots of q are

$$\mu_\pm = \frac{1}{2}\left(-e^{E_1-E_2} \pm \sqrt{e^{2E_1-2E_2} - 4e^{E_1-E_3}}\right).$$

If both roots are complex, then

$$| \mu_+ |^2 = | \mu_- |^2 = \mu_+\mu_- = e^{E_1-E_3},$$

which is less than 1.
If both eigenvalues are real,

$$\mu_+ + \mu_- = -e^{E_1-E_2},$$

which is contained in $(-1, 1)$.
Similarly as before, $q(1) > 0$, $q(-1) > 0$ (notice $1 > e^{E_1-E_2}$). Hence $\mu_\pm$ must be in $(-1, 1)$.

Chapter 4

Mean Field Theory

4.1 The Standard Approach

4.1.1 Mean Field Theory in the Ising Model

Mean Field Theory is the simplification of an inter-connected complex system by considering an average of motions of elements which are assumed to be independent [11]. Mean Field Theory gives an approximation, allowing us to qualitatively analyse the system when it is too complex to have an explicit solution. This provides a simplification of the Ising Model by taking the average of the spins, where we assume each spin to be independent. This helps in providing an analytical solution by ignoring fluctuations [15].
In our analysis using Mean Field Theory, we find the critical values beyond which phase transition occurs i.e. a sudden change by a small change in one parameter such as temperature [6].

Consider the Hamiltonian of the Ising Model (with $\sigma_j = \pm 1$)

$$-\mathcal{H}(\sigma) = J\sum_{\langle i,j\rangle}\sigma_i\sigma_j + Kh\sum_j \sigma_j.$$

We need to find an expression for the mean of the spins so that we can deduce key properties about the system. The mean is $m = \frac{1}{N}\sum_j \sigma_j$ where N is the number of lattice points. The interaction of the neighbours is

$$\sum_{\langle i,j\rangle}\sigma_i\sigma_j = \sigma_i \sum_{j\in N(i)}\sigma_j \approx zm\sigma_i,$$

where $z = N(i)$ is the number of closest neighbours of i, $z = 2d$ in d-dimensions. Now, fixing σ_i,

$$-\mathcal{H}(\sigma_i) = (Jzm + Kh)\sigma_i := h_{mf}\sigma_i,$$

where h_{mf} is the effective mean field energy given by $Jzm + Kh$.
We can also compute the configuration probabilities, $P(\sigma) \propto e^{-\beta\mathcal{H}(\sigma)}$ where $\beta = 1/\kappa T$ where κ is Boltzman's constant and T is the temperature [6]. Normalising these probabilities we now get [11],

$$m = \sum_{\sigma_i=\pm 1}\sigma_i P(\sigma_i) = \tanh(\beta h_{mf}). \tag{4.1}$$

Equation (4.1) depends on a variety of parameters and is not easily solved. An approach we can take to solve it is to Taylor expand this up to cubic order and then solve for m in terms of the other parameters, J, z, K, h, to find the conditions for which phase transition happens.
Through this method we get 3 solutions to (4.1); $m = 0$ is always a solution and the other two solutions will either be real or complex. If we can determine where exactly these solutions become real (i.e. we have 3 solutions), we can find the point at which phase transition occurs, which is dependent on the parameters.

4.1.2 Application to Gangs and Graffiti

In our investigation, we are going to use the reduced Hamiltonian from Chapter 2:

$$-\mathcal{H}_r(\underline{s}) = J_1 \sum_i \eta_i^2 + J_2 \sum_{\langle i,j \rangle} \eta_i \eta_j + J_3 \sum_{\langle\langle i,j \rangle\rangle_1} \eta_i \eta_j + J_4 \sum_{\langle\langle i,j \rangle\rangle_2} \eta_i \eta_j, \tag{4.2}$$

where

$$J_1 = \alpha + \frac{4J^2 + K^2}{4\lambda}, \;\; J_2 = \frac{JK}{\lambda}, \;\; J_3 = \frac{J^2}{2\lambda}, \;\; J_4 = \frac{J^2}{\lambda}.$$

Unlike the Ising Model,we have 3 states ($\eta_i = -1, 0, 1$) which represent territory occupied by the blue gang, neutral territory and territory occupied by the red gang respectively. Using the Mean Field Theory approach, we let

$$m = \frac{1}{N} \sum_j \eta_j$$

where we define N to be the number of points in the 2 dimensional Lattice, Λ.
Now we fix i to work out the Hamiltonian for specific points on our lattice. This gives:

$$-\mathcal{H}_r(\eta_i) = J_1 \eta_i^2 + \eta_i mz(J_2 + J_3 + J_4) = (J_1 \eta_i + mz(J_2 + J_3 + J_4))\eta_i. \tag{4.3}$$

As we have, $P(\eta) \propto e^{-\mathcal{H}(\eta)}$ (in this model, we have included any constants within the parameters so we can leave out β), we find that

$$\begin{aligned}
P(\eta_0) &= \frac{1}{1 + e^{-\mathcal{H}^+} + e^{-\mathcal{H}^-}}, \;\; \eta_0 = 0, \\
P(\eta_+) &= \frac{e^{-\mathcal{H}^+}}{1 + e^{-\mathcal{H}^+} + e^{-\mathcal{H}^-}}, \;\; \eta_+ = 1, \\
P(\eta_-) &= \frac{e^{-\mathcal{H}^-}}{1 + e^{-\mathcal{H}^+} + e^{-\mathcal{H}^-}}, \;\; \eta_- = -1.
\end{aligned}$$

By the definition of m,

$$m = \sum_i \eta_i P(\eta_i) = \frac{e^{-\mathcal{H}^+} - e^{-\mathcal{H}^-}}{1 + e^{-\mathcal{H}^+} + e^{-\mathcal{H}^-}}$$

where

$$\begin{aligned}
-\mathcal{H}^+ &= J_1 + mz(J_2 + J_3 + J_4), \\
-\mathcal{H}^- &= J_1 - mz(J_2 + J_3 + J_4).
\end{aligned}$$

This gives us:

$$m = \frac{e^{J_1} 2 \sinh(h_{mf})}{1 + e^{J_1} 2 \cosh(h_{mf})} \tag{4.4}$$

where

$$h_m f = mz(J_2 + J_3 + J_4) = mz\left(\frac{2JK + 3J^2}{2\lambda}\right),$$

$$J_1 = \alpha + \frac{4J^2 + K^2}{4\lambda},$$

where z is the number of nearest neighbours. Since we are in two dimensions, $z = 4$. Now following the procedure suggested in Section 4.1.1, we Taylor expand the right hand side of (4.4) up to the cubic term. We do this to exploit the odd nature of a cubic function. The Taylor expansion yields:

$$\frac{1}{1 + 2e^{J_1}} \left(8e^{J1} Lm + 2\left(\frac{32}{3} e^{J_1} L^3 - \frac{64(e^{J_1})^2 L^3}{1 + 2e^{J_1}}\right) m^3\right) \tag{4.5}$$

where, for simplicity, we introduce the variable L to represent $J_2 + J_3 + J_4$.
Now we can find m where (4.4) is satisfied by using the Taylor expansion found in (4.5). The solutions are:

$$m = 0, \pm\frac{1}{8} \frac{\sqrt{3}\sqrt{Le^{J_1}(-1 + 4e^{J_1})(16(e^{J_1})^2 L + 8e^{J_1} L - 4(e^{J_1})^2 - 4e^{J_1} - 1}}{L^2 e^{J_1}(-1 + 4e^{J_1})}. \tag{4.6}$$

There are 3 roots to (4.4) when the expression in the square root in (4.6) is positive. Otherwise the only solution is $m = 0$, because when we have imaginary solutions to (4.4), we cannot apply them practically. Therefore in order to find the critical parameters, we need to find the values for which the expression in the square root is positive. We first consider the boundaries i.e. where the expression in the square root is equivalent to 0 and then we will determine which regions have 1 solution and which regions have 3. We consider the real solutions given below:

$$J_1 = J_1, \qquad L = 0, \tag{4.7a}$$

$$J_1 = -2\ln 2, \qquad L = L, \tag{4.7b}$$

$$J_1 = J_1, \qquad L = \frac{1 + 2e^{J_1}}{8e^{J_1}}. \tag{4.7c}$$

Plotting the curves from (4.7) allows us to investigate each region in the real plane to see where there are 3 solutions or 1 solution. This is displayed below in Figure 4.1.

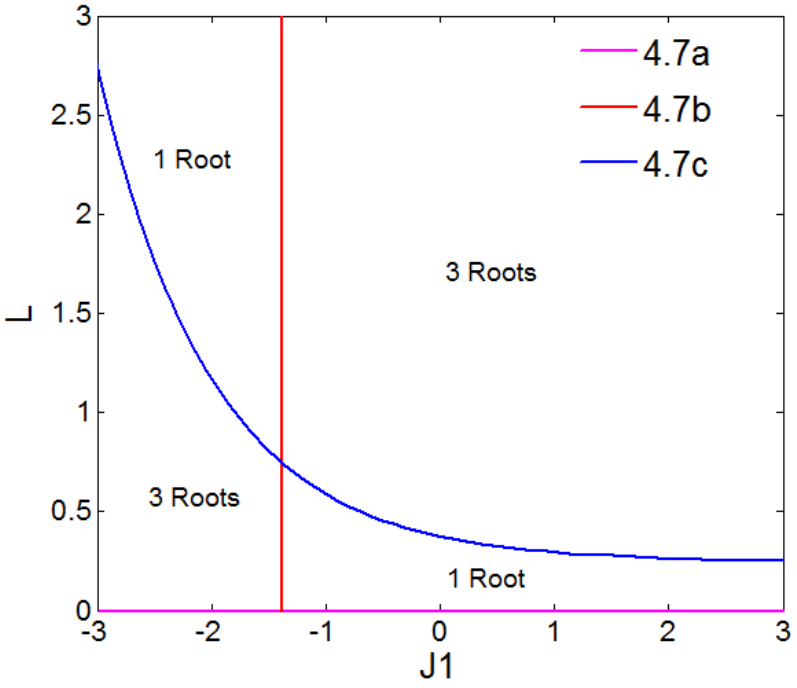

Figure 4.1: Critical Parameter Curves

Evaluating m in each region, we find the regions which give imaginary solutions and real solutions. As we progress from "3 roots" to "1 root" a phase transition has occurred. As discussed earlier, the regions with imaginary solutions give $m = 0$ as the only practical solution, which either represents no gangs or neither gang dominating the area. On the other hand in the regions with real solutions, there are 3 solutions and we have one gang dominating the other. The solutions are symmetric (we have $\pm m$), so the sign is arbitrary in representing which gang dominates.

The standard Mean Field Theory approach with one mean field variable is not well suited to our adaptation of the Ising model. We are interested in reducing the overall gang fraction as opposed to finding an equilibrium with an equal number of gangs ($m = 0$). To do this we must introduce a new variable representing gang fraction and take a different approach to Mean Field Theory pursued in the next section.

4.2 An Alternative Approach

4.2.1 Background

As discussed in the previous section, when adapting the Ising Model to gangs and graffiti, the regular Mean Field Theory approach is not entirely suitable as a mean of zero could imply that both gangs have equal control in the area. As a solution to this problem, "Territorial Developments Based on Graffiti: A Statistical Mechanics Approach" [1] introduces a new variable based on the gang fraction. We will be applying the method detailed in the paper to the reduced Hamiltonian (4.2) in the remainder of this chapter.

4.2.2 Application to the Reduced Model

Let N be the total number of lattice sites, N^+ be the number of sites occupied by the red gang and N^- be the number of sites occupied by the blue gang. We can define m, the mean and f, the fraction of sites occupied by the gangs as:

$$m = \frac{N^+ - N^-}{N}, \;\; f = \frac{N^+ + N^-}{N}.$$

It can be seen from these definitions that $0 < f < 1$ and $-f < m < f$. Proceeding further in our investigation, m and f will be our mean field variables. Instead of fixing η_i, we will fix m and f to get an equation in terms of the variables. To evaluate the number of lattice points occupied by the red gang and the blue gang (N^+ and N^- respectively), we can rearrange these equations to find:

$$N^+ = \frac{f+m}{2}N, \;\; N^- = \frac{f-m}{2}N.$$

Now we focus our attention to finding the mean field energy for fixed f and m. We are trying to find a simpler expression for the reduced Hamiltonian in terms of our mean field variables.
The first term simplifies to:

$$J_1 \sum_i \eta_i^2 = J_1(N^+ + N^-) = J_1 N f.$$

Using a similar approach to the previous section, the remaining terms simplify to:

$$J_2 \sum_{\langle i,j \rangle} \eta_i \eta_j + J_3 \sum_{\langle\langle i,j \rangle\rangle_1} \eta_i \eta_j + J_4 \sum_{\langle\langle i,j \rangle\rangle_2} \eta_i \eta_j = N(J_2 + J_3 + J_4) z m \eta_i \approx N(J_2 + J_3 + J_4) z m^2,$$

where we have approximated η_i with m because m represents the average of what the spin would be.
So we now have the following expression for the mean field energy:

$$-\mathcal{H}_r^{MF} \approx N\left(J_1 f + (J_2 + J_3 + J_4) z m^2\right). \tag{4.8}$$

We now introduce the partition function $\mathcal{Z}^{MF}$. The partition function is the sum of all the possible proportional probabilities; in other words, the normalising function. It links the different states of the system in one algebraic expression [15],

$$\mathcal{Z}^{MF} = \sum_{s} e^{-\mathcal{H}_r^{MF}(s)} = \sum_{f,m} W_N(f,m) e^{-\mathcal{H}_r^{MF}}$$

where

$$W_N(f,m) = \binom{N}{N^+, N^-}$$

is calculated using a counting argument [1].
Using the Stirling approximation

$$k! \approx \sqrt{2\pi k}\left(\frac{k}{e}\right)^k, \quad k \to \infty,$$

we can find an equivalent form of $W_N(f,m)$

$$W_N(f,m) \approx \left[\left(\frac{f+m}{2}\right)^{\frac{f+m}{2}} \left(\frac{f-m}{2}\right)^{\frac{f-m}{2}} (1-f)^{1-f}\right]^{-N}.$$

Now applying the partition function, $\mathcal{Z}^{MF}$ to our model:

$$\begin{aligned}
\mathcal{Z}^{MF} &= \sum_{f,m} W_N(f,m) e^{-\mathcal{H}_r^{MF}} \\
&\approx \sum_{f,m} e^{N(J_1 f + (J_2+J_3+J_4) z m^2)} \left[\left(\frac{f+m}{2}\right)^{\frac{f+m}{2}} \left(\frac{f-m}{2}\right)^{\frac{f-m}{2}} (1-f)^{1-f}\right]^{-N} \\
&:= \sum_{f,m} e^{-N\Phi(f,m)},
\end{aligned}$$

where we have introduced the function $\Phi(f,m)$. This is the function that represents the free energy of the system. We find that $\Phi(f,m)$ is,

$$\begin{aligned}
\Phi(f,m) = &- J_1 f - (J_2+J_3+J_4) z m^2 + \frac{f+m}{2}\log\left(\frac{f+m}{2}\right) \\
&+ \frac{f-m}{2}\log\left(\frac{f-m}{2}\right) + (1-f)\log(1-f).
\end{aligned} \tag{4.9}$$

Minimising $\Phi(f,m)$ is equivalent to finding the minimum of the energy in the system [6]. In the physical context, this means that the system has reached a steady state, i.e. a phase transition has occurred. In our adaptation of the model, this represents a decrease in the gang fraction. To find this minimum, we differentiate (4.9) with respect to f and m and set these equal to zero which gives us equations that the minimisers (f^*, m^*) satisfy. The partials are:

$$\begin{aligned}
\frac{\partial \Phi}{\partial m} &= -2mz(J_2+J_3+J_4) + \frac{1}{2}\log(f+m) - \frac{1}{2}\log(f-m) = 0, \\
\frac{\partial \Phi}{\partial f} &= -J_1 + \log(2) - \frac{1}{2}\log(f+m) - \frac{1}{2}\log(f-m) + \log(1-f) = 0.
\end{aligned}$$

Rearranging these, substituting $z = 4$ (as we are in 2 dimensions) and setting $L = J_2 + J_3 + J_4$ as before, we get

$$16mL = \log\left(\frac{f+m}{f-m}\right), \tag{4.10}$$

$$4e^{2J_1} = \frac{f^2 - m^2}{(1-f)^2}. \tag{4.11}$$

We can see from (4.10) that $m = 0$ is a solution and substituting this into (4.11) we get a solution

$$m = 0, \;\; f = \frac{2e^{J_1}}{1 + 2e^{J_1}}.$$

This solution is not necessarily unique, so taking an approach similar to the previous section, we Taylor expand the right hand side of (4.10), upto cubic terms. This gives us

$$\frac{2}{f}m + \frac{2}{3f^3}m^3.$$

Now substituting the Taylor expansion into (4.10),

$$16mL = \frac{2}{f}m + \frac{2}{3f^3}m^3.$$

Solving for m we get

$$m = 0, \pm\sqrt{24Lf - 3}f. \tag{4.12}$$

Now, we can find the region where phase transition occurs by calculating where we have three real solutions to (4.12). This gives us the condition:

$$L = \frac{1}{8f}. \tag{4.13}$$

Now solving equations (4.11) and (4.13), we get

$$L = \frac{1}{8f}, \;\; J_1 = \frac{1}{2}\log\left(\frac{1}{4}\frac{f^2 - m^2}{f^2 - 2f + 1}\right). \tag{4.14}$$

Now substituting $m = \sqrt{24Lf - 3}f$ into our equation for J_1, we have

$$J_1 = \frac{1}{2}\log\left(\frac{1}{4}\frac{f^2 - (24Lf - 3)f^2}{f^2 - 2f + 1}\right).$$

Now we can plot the conditions in (4.14) parametrically to see the boundary between 1 and 3 solutions.

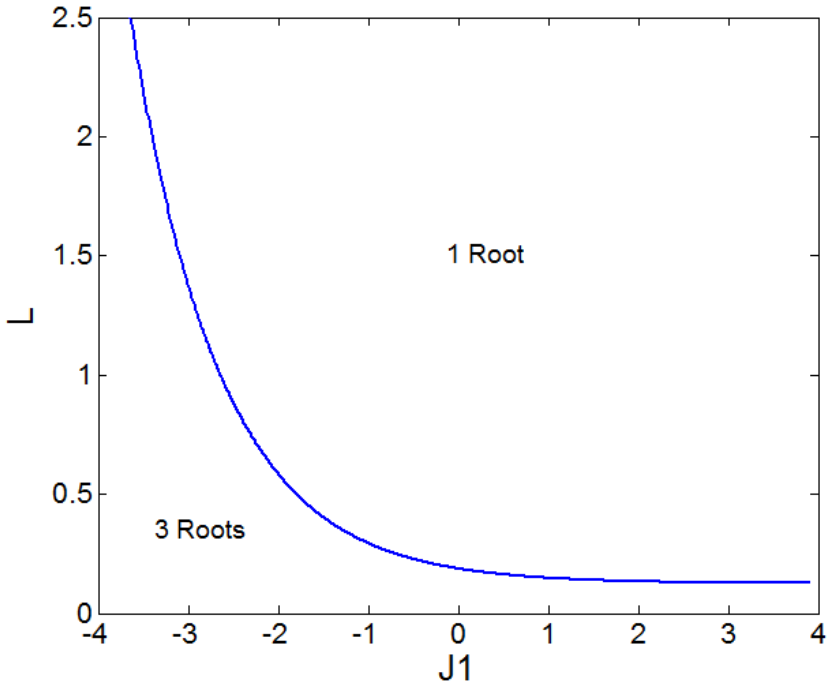

Figure 4.2: Critical Parameter Curves

Carrying out a similar analysis to the one in Section 4.1.2, we can find the regions which give imaginary solutions and those which give real solutions. We know that phase transition occurs when solutions move from the region with 3 solutions to the region with 1 solution.

Comparing Figure 4.1 to Figure 4.2, we can see similarities between the variables L and J_1. However, there are also a few differences. Firstly, Figure 4.1 had two regions with 1 solution and two regions with 3 solutions, whereas in Figure 4.2, there is only one region with 1 solution and one region with 3 solutions. Theoretically, this is because of there are fewer equations restricting the critical parameters. Introducing f, representing the gang fraction, has simplified the analysis of phase transitions. In the next chapter, we will compare the two different Mean Field Theory approaches for finding the critical parameters.

Chapter 5

Simulations

We will now compare our findings from Mean Field Theory to simulations to see points of phase transition. For simplicity we will consider the case where $J = 1$ (neighbouring agents are likely to align with each other), $K = 1$ (gangs are likely to occupy areas which have been marked by their own gang) and focus our attentions to α (gang aggressiveness) and λ (social influence), to see how much policing is needed to control varying degrees of gang aggressiveness. We will quantitatively compare the phase transitions in the simulations for constant J, K to the critical parameters found in Chapter 4.

5.1 Phase Transition

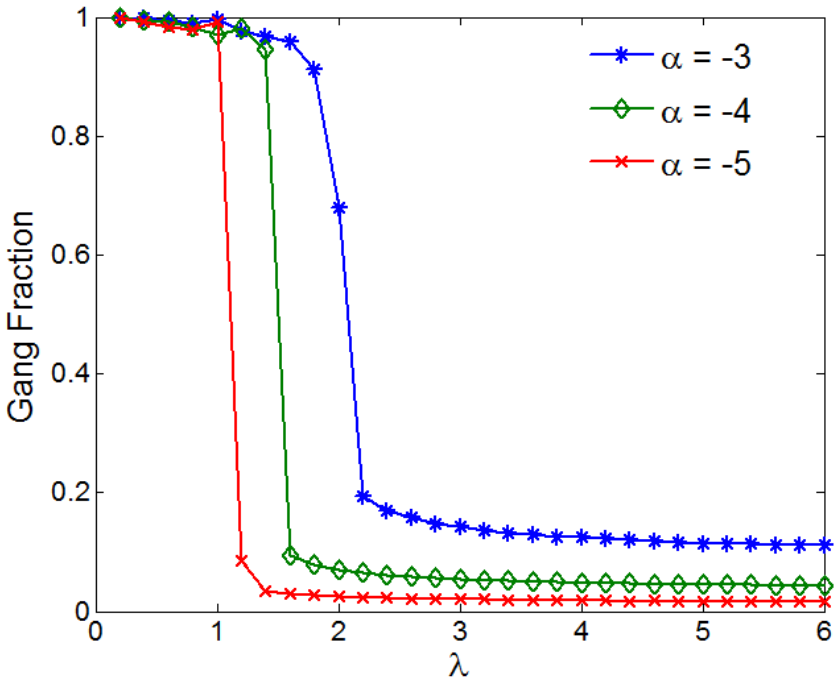

Figure 5.1: Fraction of gang members for fixed α

The plot, Figure 5.1 shows the corresponding critical value of λ for each α by simulating using Markov Chain Monte Carlo (MCMC) methods. Our observations were:

- Increasing α moves the curve further to the right. From this we can deduce that for high α we need higher λ to achieve a phase transition, which makes sense intuitively. In the physical context this implies that to match the higher aggression shown by the gangs, the positive influence of society needs to be increased (that is, more policing is required) to achieve the desired lower gang fraction.
- For smaller α, the drop in gang fraction is more abrupt. This means that for lower gang aggressiveness a smaller increase in positive social influence (λ) is required to decrease the gang fraction in the area. This makes sense as for less aggressive gangs, a smaller change in policing would be required to decrease the gang fraction.

We will now compare this result to our findings from applying the standard Mean Field Theory approach in Section 4.1.2. The table below lists critical parameters $[\alpha, \lambda]$ when the Mean Field Theory approach is used.

$\boldsymbol{\alpha}$	$\boldsymbol{\lambda}$
-3	1.7140
-4	1.6022
-5	0.7163

Table 5.1: Critical Values from Mean Field Theory

Inspecting the results in Table 5.1, we notice a similar correlation between α and λ - i.e. if there is an increase in the level of gang aggressiveness (higher α), more positive societal influence is required in order to obtain low gang activity (i.e. higher λ). Comparing these values with the values in Figure 5.1, upon fixing α at -3,-4,-5 the critical value of λ obtained using Mean Field Theory is approximately the same.

A key point to note, however is that there is a slight disparity between the critical $[\alpha, \lambda]$ depending on the different methods used, which can be explained using the theory of each technique.

- The simulations are random and probabilistic which only gives us an estimation of where phase transition occurs.
- Applying the Mean Field Theory approach an approximate Taylor expansion is used which reduces the accuracy, albeit slightly.

In addition it is important to note that the disparity does not have a correlation with the value of α, so it could be left completely to randomness. For confirmation we would have to test this assumption by studying the results for different fixed values of α.

Now as we deduced in Section 4.1.2, while the Mean Field Theory approach gives us values of critical α and λ, it does not necessarily suggest anything about the gang fraction. Hence it would be more useful to consider the adapted Mean Field Theory approach from Section 4.2 which also involves a calculation of f representing the gang fraction. The table below shows the critical $[\alpha, \lambda]$ as well as the gang fraction, f, at the point of phase transition.

α	λ	f
-3	2.7227	0.1361
-4	1.5308	0.0765
-5	0.9529	0.0476

Table 5.2: Critical Values from the second approach

Firstly, we compare the critical values for $[\alpha, \lambda]$ from the two different mean field approaches. We can see that both approaches give different critical values of λ for fixed α. There is not a definitive trend between the 2 different sets of values for λ. The differences are most likely due to the introduction of the new variable f, as it affects the mean. A reasonable deduction to make is that the second Mean Field Theory approach provides a better estimate. Comparing these values to the ones in the simulation diagram, the λ values at phase transition for each of the $\alpha's$ are better matched using the second Mean Field Theory approach (Table 5.1).

We now consider the graphical representation of our finding in Section 4.2.2, plotting the following graph where $f = \dfrac{2e^{J_1}}{1 + 2e^{J_1}}$:

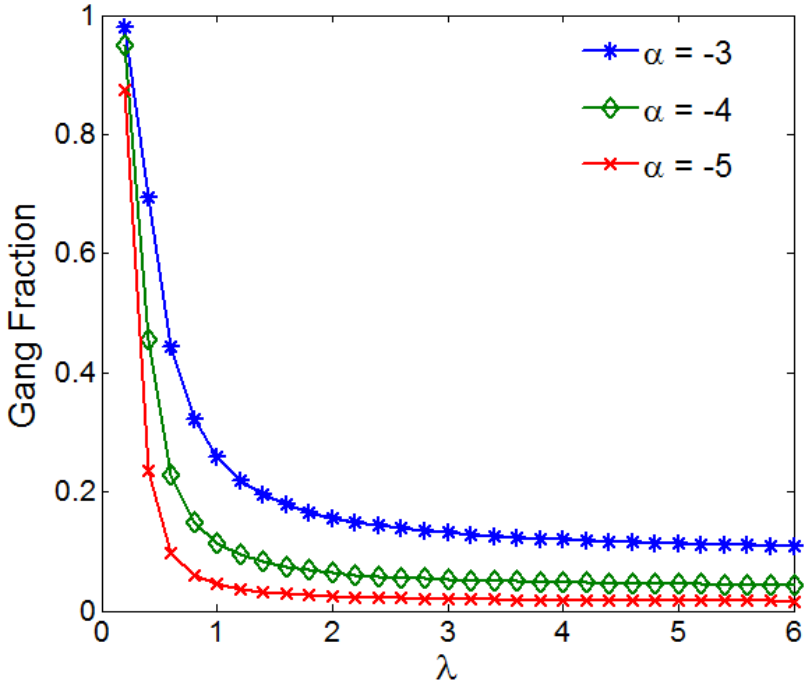

Figure 5.2: Fraction of gang members using MFT

The main purpose behind using the second Mean Field Theory approach was that it enabled us to calculate the gang fraction, f. Comparing the f-values in Figure 5.2 to the gang fraction from the point of phase transition in Figure 5.1, we see that the fraction is very similar. However before the model reaches its steady state, the gang fraction in Figures 5.1 and 5.2 do not match up. Considering the fact that we have used a Taylor expansion when using Mean Field Theory, this is not surprising, as greater values of m will have lower accuracy.
We deduce:

- Figure 5.2 confirms that the Second Mean Field theory approach gives us a better understanding of the Ising Model applied to gangs and graffiti.
- Table 5.1 shows that for lower α, the critical λ achieves a lower gang fraction. In the physical context, this makes sense as lower levels of gang aggressiveness would suggest lower gang fractions.
- Overall, in both Mean Field Theory approaches and the simulations we see that to combat gang activity when there is higher gang aggression (α), we need more positive social influence/higher policing (λ).

5.2 Gang Fraction

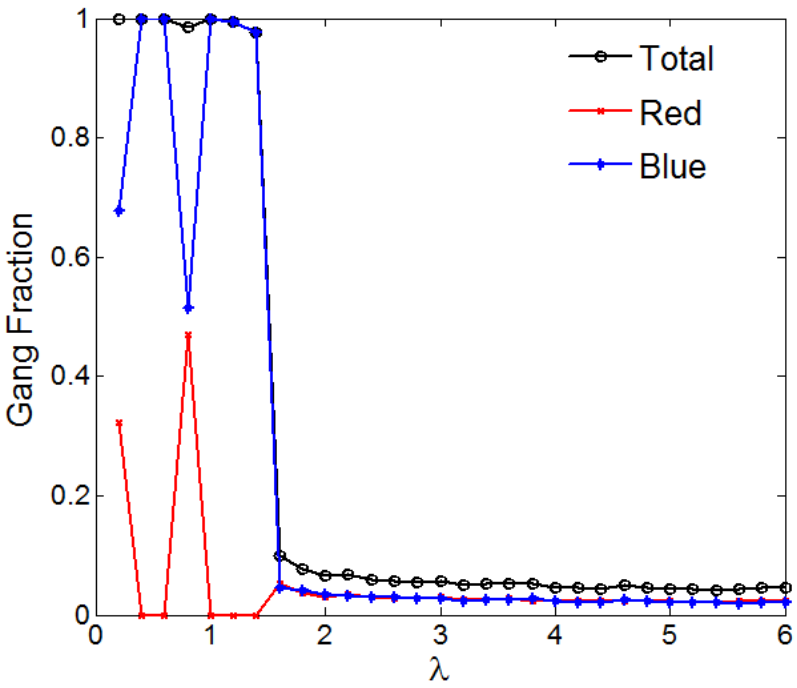

Figure 5.3: Fraction of gang members for $\alpha = -4$

Figure 5.3 is another way to display the information provided from the simulations in Figure 5.1. Figure 5.3 shows the control of each gang as well as the overall gang fraction for a fixed value, $\alpha = -4$. As expected, at the point of the phase transition, the total gang fraction drops to approximately 0.1 as we saw in Table 5.1 and Figure 5.1. Another point to note is that before phase transition occurs, there are fluctuations in gang control where in this case the blue gang dominates with a much higher gang fraction. The domination of the blue gang over the red is the result of the arbitrary initial values of the simulation. The change in gang fraction of each gang, however, is to be expected as there would be multiple changes in dominance before one of the gangs finally takes control of the area in the steady state.

5.3 Energy of the System

We can calculate the energy in the system (i.e. the Hamiltonian $\mathcal{H}$) and compare this to our theory about phase transitions. As in Section 5.2 we represent the findings for the value $\alpha = -4$.

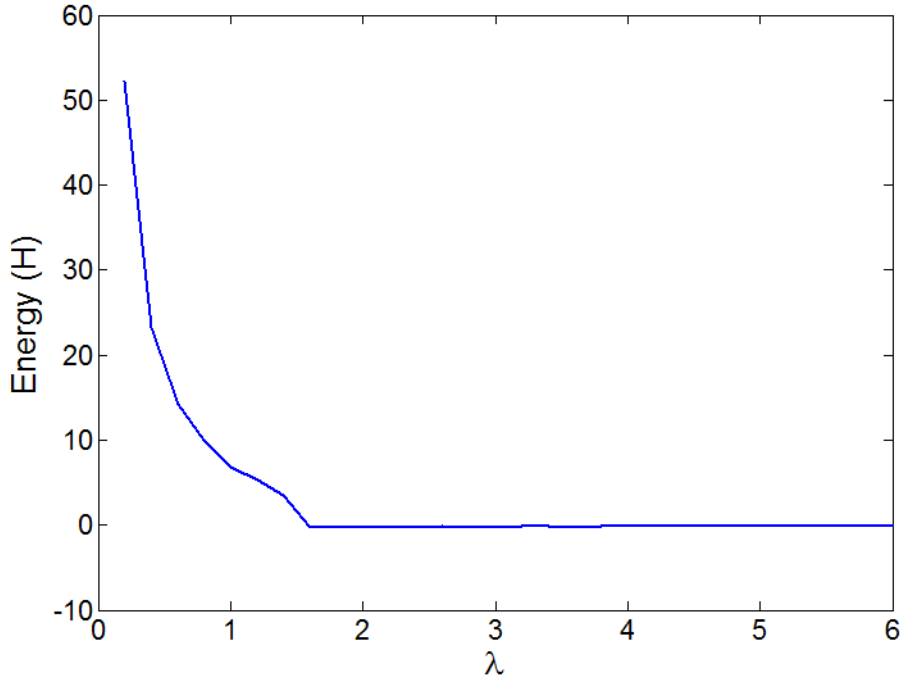

Figure 5.4: Energy of the system for $\alpha = -4$

As in Chapter 2, when the model reaches its steady state the energy is minimised. Beyond this point, changing λ does not affect the energy levels as we have reached the lowest possible gang fraction in the area. This confirms our assumption in Chapter 4 that minimising the free energy function (Φ) leads to the critical parameters for phase transition.

Chapter 6

Conclusion

In this project, we applied various techniques to our adaptation of the Ising model representing the interaction between gangs and graffiti. We used Markov Chain transition matrices and Mean Field Theory. We then compared our theory to simulations to see the usefulness of the approaches.

When applying Markov Chain transition matrices, we managed to extend the algorithm to three energy states and showed that there could be multiple possible transition matrices when we are considering three energy states. For specific values of E_1, E_2, E_3 we would be able to find an optimal transition matrix by evaluating the remaining eigenvalues and choosing the matrix with the eigenvalues with the smallest absolute value to use in our code. Cases where the energies of different states are the same can be ignored because this is highly unlikely in practical applications.

Using the Mean Field Theory approximation we deduced the set of critical parameters and displayed them graphically. We adapted the standard Mean Field Theory approach to include two variables enabling us to study the gang fraction alongside the mean. This method proved to be quite successful as it helped finding where phase transition occurs. We found that higher levels of gang aggressiveness required a more positive societal influence. In our adaptation of Mean Field Theory we used the Taylor expansion. An alternative approach would be to do various plots using the closed form of the function we obtained. This could give us a better estimate as there would not be the error from truncating the Taylor expansion.

In the Simulations chapter, we successfully found how varying the policing in the area minimises the gang fraction by adapting our theory in the case $J = K = 1$ for values of α. Running more simulations for varied J, K and a larger range of values of α could give greater insight into gang behaviour; where we can continue to use the second Mean Field Theory approximation to obtain a better understanding.

Overall, the model could be improved in a few ways so that it better fits the interaction between gangs and graffiti. In our model we assume that both gangs have the same level of aggressiveness. An improvement would be to take into account the aggressiveness of each gang individually. Also, in the current model we study the interaction of 2 gangs - we could adapt this to include more gangs. Another area of further study would be working towards incorporating the lattice structure to more complicated shapes which are better approximations of maps of areas.

Bibliography

[1] A. Barbaro, L. Chayes, and M. R. D'Orsogna. Territorial Developments Based on Graffiti: A Statistical Mechanics Approach. *Physica A: Statistical Mechanics and its Applications*, 392(1), 2013.

[2] Ayouche O., Lau E., Liu W., and Magli A. Ising Model for Gangs and Graffiti. Second Year Group Project, Imperial College London, 2014.

[3] *http://aux.shenkar.ac.il/2014/group17/World_ americas.html*, [Accessed 17 June 2015].

[4] UK Essays. *Youth Gang Culture and Publics Perception Of Gangs Criminology Essay [Internet]*, November 2013. [Accessed 17 June 2015].

[5] Peter Byrne. *Rioting in Toxteth, Liverpool http://www.theguardian.com/info/2011/dec/15/reading-the-riots-ebook*, [Accessed 17 June 2015].

[6] Barry A. Cipra. An Introduction to the Ising Model. *Am. Math Monthly*, 94(10), December 1987.

[7] Giovanni Gallavotti. *Statistical Mechanics: A Short Treatise*. Springer, Berlin, 1999.

[8] L. Onsager. Crystal Statistics I. A Two-dimensional Model with an Order-Disorder Transition. *Physical Review*, 65(3-4), 1944.

[9] J. M. Yeomans. *Statistical Mechanics of Phase Transitions*. Oxford University Press, Oxford, 1992.

[10] Wei Cai. Handout 12. Ising Model. Stanford University, ME346A Introduction to Statistical Mechanics Lecture Handout, 2011.

[11] Shang-Keng Ma translated by M. K. Fung. *Statistical Mechanics*. World Scientific Publishing Co Pte Ltd., Philadelphia, 1985.

[12] Dani Gamerman and Hedibert F. Lopes. *Markov Chain Monte Carlo*. Chapman & Hall/CRC, Taylor & Francis Group, Florida.

[13] M. E. J. Newman and G. T. Barkema. *Monte Carlo Methods in Statistical Physics*. The Clarendon Press, Oxford University Press, New York, 1999.

[14] Yanghong Huang. Email communication with Alina Leidinger and Sanjiv Dutt, 8 June 2015.

[15] Kim Christensen and Nicholas R Moloney. *Complexity and Criticality*. Imperial College Press, London, 2005.

Appendix A

Code

Below are the three programs we used and adapted for our simulations.

A.1 Main Function to Calculate Gang Fractions

```
function [eqE, Gfrac] = Gangfrac(J,K,alpha,lambda)

% For each parameter J, K, alpha and lambda, return the energy eqE and the
% fraction of Gang Gfrac (including both fractions)

N = 100;  % Size of the lattice N by N
RN = 40; % Number of sweeps RN*RN per iteration
MaxIter = 2000;

% Turn of the following line once it is run once
mex mex_RedGangMetrop.c

% Parameters in the reduced model
J1 = alpha+J^2/lambda+K^2/4/lambda;
J2 = J*K/lambda;
J3 = J^2/2/lambda;
J4 = J^2/lambda;

% Initial configuration for the grid
s = zeros(N+4,N+4);
s(3:N+2,3:N+2) = floor(3*rand(N,N))-1; % Random initial data
s = RedPeriodComp(s,N);

% Data to save at each iteration
myE = [];  % Energy
myM = [];  % The average gang fraction

for iter=1:MaxIter
    ri = ceil(N*rand(2,RN*RN)); % The random site
    pi = rand(1,RN*RN);         % Random probability
    pn = randn(1,RN*RN);        % Random normal for graffiti
    mex_RedGangMetrop(RN,N,J1,J2,J3,J4,s,ri,pi);
    % Save the data per iteration
```

```
    E = J1*sum(sum(s(3:N+2,3:N+2).^2)) ...
        +J2*sum(sum(s(3:N+2,3:N+2).*(s(2:N+1,3:N+2)+s(4:N+3,3:N+2)+s(3:N
            +2,2:N+1)+s(3:N+2,4:N+3)))) ...
        +J3*sum(sum(s(3:N+2,3:N+2).*(s(1:N,3:N+2)+s(5:N+4,3:N+2)+s(3:N
            +2,1:N)+s(3:N+2,5:N+4)))) ...
        +J4*sum(sum(s(3:N+2,3:N+2).*(s(2:N+1,2:N+1)+s(2:N+1,4:N+3)+s(4:N
            +3,2:N+1)+s(4:N+3,4:N+3))));
    myE = [myE -E/N^2];
    myM = [myM; sum(sum(abs(s(2:N+1,2:N+1))))/N^2 sum(sum(s(2:N+1,2:N+1)
        >0.5))/N^2 sum(sum(s(2:N+1,2:N+1)<-0.5))/N^2];
end


% Average over the second half of the iteration
StartIter = round(MaxIter/2);
eqE = mean(myE(StartIter:MaxIter));
Gfrac = mean(myM(StartIter:MaxIter,:));
```

A.2 C Code to run the Metropolis Algorithm

```
#include "mex.h"
#include <math.h>

void mexPointPeriodicUpdate(double *s, const int i, const int j, const int
    N) {
    if (i==2 || i==3) {
        if (j==2 || j==3) {    /* south west corner */
            s[(j+N)*(N+4)+i+N] = s[j*(N+4)+i];
            s[j*(N+4)+i+N]     = s[j*(N+4)+i];
            s[(j+N)*(N+4)+i]   = s[j*(N+4)+i];
        } else if (j==N || j==N+1) {  /* south east corner */
            s[(j-N)*(N+4)+i+N] = s[j*(N+4)+i];
            s[(j-N)*(N+4)+i]   = s[j*(N+4)+i];
            s[j*(N+4)+i+N]          = s[j*(N+4)+i];
        } else          /* south interior  */
            s[j*(N+4)+i+N]     = s[j*(N+4)+i];
    } else if (i==N || i==N+1) {
        if (j==2 || j==3) {  /* north west */
            s[(j+N)*(N+4)+i-N] = s[j*(N+4)+i];
            s[j*(N+4)+i-N]     = s[j*(N+4)+i];
            s[(j+N)*(N+4)+i]   = s[j*(N+4)+i];
        } else if (j==N || j==N+1) { /* north east */
            s[(j-N)*(N+4)+i-N] = s[j*(N+4)+i];
            s[(j-N)*(N+4)+i]   = s[j*(N+4)+i];
            s[j*(N+4)+i-N]          = s[j*(N+4)+i];
        } else  /* north interior */
            s[j*(N+4)+i-N]     = s[j*(N+4)+i];
    } else {
        if (j==2 || j==3) /* west interior */
            s[(j+N)*(N+4)+i] = s[j*(N+4)+i];
        else if (j==N || j==N+1) /* east interior */
            s[(j-N)*(N+4)+i] = s[j*(N+4)+i];
    }
}

void sort3(const double *dE, double *newdE, int *ind) {
```

```
36      /* sort the 1*3 array dE, and keep the index
37         because of the small size, we can discuss all six cases*/
38      if (dE[0] < dE[1]) {
39          if (dE[2] < dE[0]) {
40              newdE[0] = dE[2]; newdE[1] = dE[0]; newdE[2] = dE[1];
41              ind[0] = 2; ind[1] = 0; ind[2] = 1;
42          } else {
43              if (dE[2] < dE[1]) {
44                  newdE[0] = dE[0]; newdE[1] = dE[2]; newdE[2] = dE[1];
45                  ind[0] = 0; ind[1] = 2; ind[2] = 1;
46              } else {
47                  newdE[0] = dE[0]; newdE[1] = dE[1]; newdE[2] = dE[2];
48                  ind[0] = 0; ind[1] = 1; ind[2] = 2;
49              }
50          }
51      } else {
52          if (dE[2] < dE[1]) {
53              newdE[0] = dE[2]; newdE[1] = dE[1]; newdE[2] = dE[0];
54              ind[0] = 2; ind[1] = 1; ind[2] = 0;
55          } else {
56              if (dE[0] < dE[2]) {
57                  newdE[0] = dE[1]; newdE[1] = dE[0]; newdE[2] = dE[2];
58                  ind[0] = 1; ind[1] = 0; ind[2] = 2;
59              } else {
60                  newdE[0] = dE[1]; newdE[1] = dE[2]; newdE[2] = dE[0];
61                  ind[0] = 1; ind[1] = 2; ind[2] = 0;
62              }
63          }
64      }
65      return;
66  }
67
68  /* Find the indices of nonzero element*/
69  int find3(const int *ind, const double sij) {
70      int current_ind;
71      if (ind[0]==sij+1)
72          current_ind = 0;
73      else if (ind[1]==sij+1)
74          current_ind = 1;
75      else if (ind[2]==sij+1)
76          current_ind = 2;
77      else {
78          mexPrintf("Error!\n");
79          exit(0);
80      }
81      return current_ind;
82  }
83
84  /* Metropolis algorithm using C, to increase the speed
85   * mex_RedGangMetrop(RN,N,J1,J2,J3,J4,s,rand_int,prob);
86   */
87  void mexFunction(int nlhs, mxArray *plhs[], int nrhs, const mxArray *prhs
        [])
88  {
89      int RN, N;
90      double J1, J2, J3, J4;
91      double *s, *rand_int, *prob;
```

```
92
93      int i, j, k;
94      double temp, dE[3], newdE[3];
95      int ind[3];
96      int current_ind;
97
98      RN = mxGetScalar(prhs[0]);
99      N = mxGetScalar(prhs[1]);
100     J1 = mxGetScalar(prhs[2]);
101     J2 = mxGetScalar(prhs[3]);
102     J3 = mxGetScalar(prhs[4]);
103     J4 = mxGetScalar(prhs[5]);
104     s  = mxGetPr(prhs[6]);
105     rand_int = mxGetPr(prhs[7]);
106     prob = mxGetPr(prhs[8]);
107
108     for (k=0; k<RN*RN; k++) {
109         /* choose the random site */
110         i = (int)rand_int[2*k-2]+1;
111         j = (int)rand_int[2*k-1]+1;
112         /* calculate the three energyies for the three gang states
               (-1,0,1) */
113         temp = J2*(s[(j+1)*(N+4)+i]+s[(j-1)*(N+4)+i]+s[j*(N+4)+i+1]+s[j*(N
               +4)+i-1])
114               + J3*(s[(j+2)*(N+4)+i]+s[(j-2)*(N+4)+i]+s[j*(N+4)+i+2]+s[j*(N
                   +4)+i-2])
115               + J4*(s[(j+1)*(N+4)+i+1]+s[(j+1)*(N+4)+i-1]+s[(j-1)*(N+4)+i
                   +1]+s[(j-1)*(N+4)+i-1]);
116         dE[0] = -J1+temp; dE[1] = 0; dE[2] = -J1-temp;
117         sort3(dE,newdE,ind); /* sort the energy and update according to
               their energy difference*/
118         current_ind = find3(ind,(int)s[j*(N+4)+i]); /* Find the index of
               the current energy*/
119         if (current_ind==0) { /* lowest energy */
120             if (prob[k]<exp(newdE[0]-newdE[1]))
121                 s[j*(N+4)+i] = ind[1]-1;
122         } else if (current_ind==1) {
123             if (prob[k]<exp(newdE[1]-newdE[2]))
124                 s[j*(N+4)+i] = ind[2]-1;
125             else
126                 s[j*(N+4)+i] = ind[0]-1;
127         } else
128             s[j*(N+4)+i] = ind[0]-1;
129         mexPointPeriodicUpdate(s,i,j,N);
130     }
131 }
```

A.3 Part of the Code for the Initial Configuration of the Grid

```
1 function s_out = RedPeriodComp(s_in,N)
2
3 s_out = s_in;
4
5 s_out(1,3:N+2) = s_in(N+1,3:N+2);
```

```
6  s_out(2,3:N+2) = s_in(N+2,3:N+2);
7  s_out(N+3,3:N+2) = s_in(3,3:N+2);
8  s_out(N+4,3:N+2) = s_in(4,3:N+2);
9
10 s_out(3:N+2,1) = s_in(3:N+2,N+1);
11 s_out(3:N+2,2) = s_in(3:N+2,N+2);
12 s_out(3:N+2,N+3) = s_in(3:N+2,3);
13 s_out(3:N+2,N+4) = s_in(3:N+2,4);
14
15
16 s_out(1,1) = s_out(N+1,N+1);
17 s_out(1,2) = s_out(N+1,N+2);
18 s_out(2,1) = s_out(N+2,N+1);
19 s_out(2,2) = s_out(N+2,N+2);
20
21 s_out(N+3:N+4,1:2) = s_out(1:2,1:2);
22 s_out(1:2,N+3:N+4) = s_out(1:2,1:2);
23 s_out(N+3:N+4,N+3:N+4) = s_out(1:2,1:2);
```